


Ultra-high-field magnetic resonance spectroscopy in non-alcoholic fatty liver disease: Novel mechanistic and diagnostic insights of energy metabolism in non-alcoholic steatohepatitis and advanced fibrosis

Stefan Traussnigg¹  | Christian Kienbacher¹ | Martin Gajdošík^{2,3} | Ladislav Valkovič^{2,3,4} | Emina Halilbasic¹ | Judith Stift⁵ | Christian Rechling¹ | Harald Hofer¹ | Petra Steindl-Munda¹ | Peter Ferenci¹ | Fritz Wrba⁵ | Siegfried Trattnig^{2,3} | Martin Krššák^{2,3,6} | Michael Trauner¹

¹Division of Gastroenterology and Hepatology, Department of Internal Medicine III, Medical University of Vienna, Vienna, Austria

²High-Field MR Center, Department of Biomedical Imaging and Image-guided Therapy, Medical University of Vienna, Vienna, Austria

³Christian Doppler Laboratory for Clinical Molecular MR Imaging, Vienna, Austria

⁴Department of Imaging Methods, Institute of Measurement Science, Slovak Academy of Sciences, Bratislava, Slovakia

⁵Department of Clinical Pathology, Medical University of Vienna, Vienna, Austria

⁶Division of Endocrinology and Metabolism, Department of Internal Medicine III, Medical University of Vienna, Vienna, Austria

Correspondence

Michael Trauner, MD, Division of Gastroenterology and Hepatology, Department of Internal Medicine III, Medical University of Vienna, Vienna, Austria.
Email: michael.trauner@meduniwien.ac.at

Funding information

The research leading to these results has been partly funded by the European Union Seventh Framework Programme (/FP7/2007-2013)/ UNDER/GRANT AGREEMENT/N° HEALTH-F2-2009-241762, for the project FLIP, grant F3008-B05 from the Austrian Science Foundation (FWF) and grant LS12-008 from the Vienna Science and Technology Fund

Handling Editor: Luca Valenti

Abstract

Background & Aims: With the rising prevalence of non-alcoholic fatty liver disease (NAFLD) and steatohepatitis (NASH) non-invasive tools obtaining pathomechanistic insights to improve risk stratification are urgently needed. We therefore explored high- and ultra-high-field magnetic resonance spectroscopy (MRS) to obtain novel mechanistic and diagnostic insights into alterations of hepatic lipid, cell membrane and energy metabolism across the spectrum of NAFLD.

Methods: MRS and liver biopsy were performed in 30 NAFLD patients with NAFL (n=8) or NASH (n=22). Hepatic lipid content and composition were measured using 3-Tesla proton (¹H)-MRS. 7-Tesla phosphorus (³¹P)-MRS was applied to determine phosphomonoester (PME) including phosphoethanolamine (PE), phosphodiester (PDE) including glycerophosphocholine (GPC), phosphocreatine (PCr), nicotinamide adenine dinucleotide phosphate (NADPH), inorganic phosphate (Pi), γ -ATP and total phosphorus (TP). Saturation transfer technique was used to quantify hepatic ATP flux.

Abbreviations: ATP, adenosine triphosphate; BMI, body mass index; CSI, chemical shift imaging; ER, endoplasmic reticulum; FA, fatty acid; F_{ATP} , forward exchange flux; FOV, field of view; GPC, glycerophosphocholine; GPE, glycerophosphoethanolamine; k, exchange rate constant; HDL, high density lipoprotein; MRS, magnetic resonance spectroscopy; MUI, monounsaturate index; NADPH, nicotinamide adenine dinucleotide phosphate; NAFL, non-alcoholic fatty liver; NAFLD, non-alcoholic fatty liver disease; NASH, non-alcoholic steatohepatitis; PCr, phosphocreatine; PDE, phosphodiester; PE, phosphoethanolamine; Pi, inorganic phosphate; PME, phosphomonoester; PNPLA3, patatin-like phospholipase domain-containing protein 3; PRESS, point resolved spectroscopy; PUFA, polyunsaturated fatty acid; PUI, polyunsaturation index; SI, saturation index; TM6SF2, transmembrane 6 superfamily 2; TP, total phosphorus; VOI, volume of interest; WHR, waist-to-hip ratio.

This is an open access article under the terms of the Creative Commons Attribution-NonCommercial-NoDerivs License, which permits use and distribution in any medium, provided the original work is properly cited, the use is non-commercial and no modifications or adaptations are made.

© 2017 The Authors *Liver International* Published by John Wiley & Sons Ltd

Results: Hepatic steatosis in ^1H -MRS highly correlated with histology ($P < .001$) showing higher values in NASH than NAFL ($P < .001$) without differences in saturated or unsaturated fatty acid indices. PE/TP ratio increased with advanced fibrosis (F3/4) ($P = .002$) whereas GPC/PME+PDE decreased ($P = .05$) compared to no/mild fibrosis (F0-2). γ -ATP/TP was lower in advanced fibrosis ($P = .049$), while PCr/TP increased ($P = .01$). NADPH/TP increased with higher grades of ballooning ($P = .02$). Pi-to-ATP exchange rate constant ($P = .003$) and ATP flux ($P = .001$) were lower in NASH than NAFL.

Conclusions: Ultra-high-field MRS, especially saturation transfer technique uncovers changes in energy metabolism including dynamic ATP flux in inflammation and fibrosis in NASH. Non-invasive profiling by MRS appears feasible and may assist further mechanistic and therapeutic studies in NAFLD/NASH.

KEYWORDS

adenosine triphosphate flux, fatty liver, lipotoxicity, mitochondrial function, saturation transfer

1 | INTRODUCTION

Non-alcoholic fatty liver disease (NAFLD) has gradually become a wide spread disease affecting 40-50% of the general population¹ with serious hepatic outcomes including progression of non-alcoholic steatohepatitis (NASH) to advanced fibrosis, cirrhosis and hepatocellular carcinoma (HCC). Liver biopsy still serves as reference standard in the diagnosis of NASH but is afflicted with major drawbacks such as feasibility, sampling error, intra- and interobserver variability and potential complications² also lacking a functional in-vivo assessment. Therefore, non-invasive tools to monitor severity and progression of NAFLD are urgently needed.

Proton (^1H)- and phosphorus (^{31}P)-MR spectroscopy (MRS) might allow a non-invasive and real-time detection of hepatic fat, cell membrane and energy metabolism.^{3,4} 3 Tesla (T) ^1H -MRS is an effective tool to quantify liver steatosis⁵ and assess hepatic lipid composition.⁶ Data from ^{31}P - and carbon-13 (^{13}C)-MRS on hepatic energy⁷ and hepatic oxidative metabolism⁸ have already shown the utility evaluating the important role of the liver in the general regulation of glucose and lipid metabolism. However, most of the previously published studies on ^{31}P -MRS in NAFLD were limited to magnetic field strengths of 3 T or lower.^{9,10} Higher magnetic field strengths result in an increased signal-to-noise ratio and higher spectral resolution, which is of particular importance for ^{31}P -MRS.¹¹ We therefore explored the potential of high field 3 T ^1H and ultra-high field 7 T ^{31}P -MRS as a non-invasive tool in NAFLD patients to obtain (i) novel mechanistic insights of lipid, cell membrane and energy homeostasis in NAFLD and, (ii) novel imaging biomarkers of disease severity and progression including endoplasmic reticulum (ER) stress. In addition, we determined the rs738409 [G] polymorphism of patatin-like phospholipase domain-containing protein 3 (PNPLA3) and the transmembrane 6 superfamily 2 (TM6SF2) rs58542926 variants associated with liver steatosis, progression of liver disease and its complications,¹²⁻¹⁴ which has not been explored in the context of MRS so far.

Key points

- Saturation transfer including dynamic ATP flux is significant lower in NASH than NAFL.
- Higher ratios of PCr/TP and lower ratios of γ ATP/TP support data on apparent mitochondrial defects in NASH.
- Ultra-high field MRS leads to shorter acquisition times and may therefore improve clinical applicability.
- Poly- to monounsaturated fatty acid indices were significantly higher in non-obese (BMI < 30) than obese (BMI > 30) NAFLD patients.

2 | PATIENTS AND METHODS

2.1 | Study design

This was a prospective, non-randomized feasibility study of high field ^1H - and ultra-high field ^{31}P -MRS as a novel and non-invasive tool for the assessment of NAFLD. It was approved by the ethics committees of the *Medical University Vienna* and the *Vienna General Hospital* (2011/129). All patients provided written informed consent.

2.2 | Subjects

Subjects scheduled for routine liver biopsy with suspected NAFLD were recruited from the NAFLD outpatient clinic of the *Medical University Vienna* (Figure 1). Histological assessment was performed by two board certified pathologists (JS, FW) unaware of the MRS data serving as reference standard for the diagnosis of NAFL, NASH, severity of inflammation and fibrosis (see below). Moreover, we collected comprehensive medical history and clinical data including physical examination, liver biochemistry, glycaemic parameters and lipid profiles (Table 1).

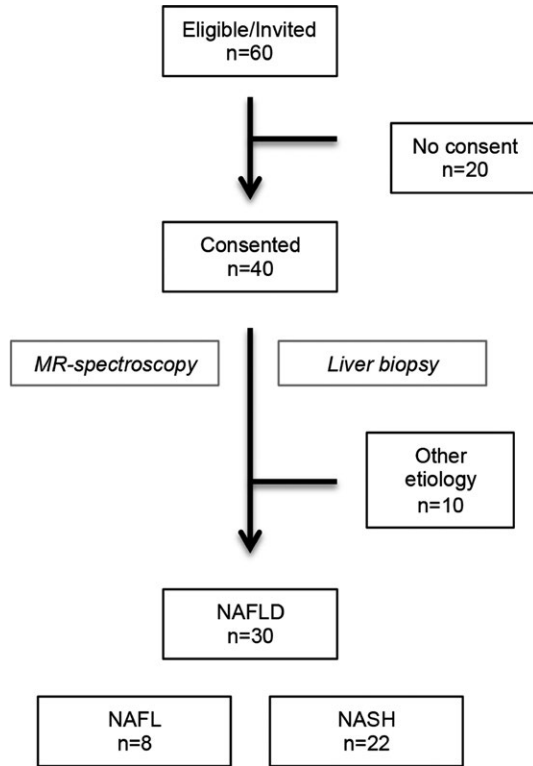


FIGURE 1 Patient selection patients were invited to participate in this study if liver biopsy was planned in suspected non-alcoholic fatty liver disease (NAFLD) patients and magnetic resonance eligibility was confirmed. After obtaining consent patients were further selected when liver biopsy showed NAFLD non-alcoholic fatty liver or non-alcoholic steatohepatitis as single diagnosis

2.3 | Inclusion and exclusion criteria

Patients had to be between 18 and 70 years old and scheduled for liver biopsy with suspected NAFLD. Exclusion criteria were as followed: (i) established chronic liver diseases other than NAFLD (ie, viral hepatitis, autoimmune liver disease, hereditary hemochromatosis, alpha-1-antitrypsin deficiency, Wilson's disease, alcoholic liver disease and cholestatic liver diseases). Patients were excluded in case of: (ii) daily alcohol consumption >30 g in males and >20 g in females, (iii) age <18 years, (iv) acute diseases within the last 2 weeks before the investigation, (v) severe or untreated heart, kidney, lung and blood disease (eg, heart failure NYHA III or IV, CKD stage >2, COPD Gold >2, any haematopoietic or lymphoid malignancy), (vi) current unstable thyroid disease, (vii) pregnancy, (viii) contraindications to MRS or liver biopsy.

2.4 | Genetic testing

Single nucleotide polymorphisms rs738409 (PNPLA3) and rs58542926 (TM6SF2) were analyzed using the StepOnePlus Real Time PCR Systems (Applied Biosystems; Foster City, CA, USA) with a TaqMan SNP Genotyping Assay developed together with Applied Biosystems using published sequences from the NCBI Entrez SNP Database.

TABLE 1 Baseline characteristics of the patient population

	NAFL (n=8)	NASH (n=22)
Male (%)	3 (38%)	15 (68%)
Age ^a (years)	48.0±9.6	48.0±12.5
Diabetes	0 (0)	8 (36) ^{b,*}
BMI ^a	27.3±5.2	31.4±4.1*
WHR ^a	0.90±0.05	0.98±0.07**
Non-obese (BMI<30)	6 (75%)	10 (45%)
PNPLA3		
CC/GC	5/3	9/7
GG	0	6**
TM6SF2		
CC	7	18
CT	1	3
TT	0	1
AST ^a (IU/L)	38.1±14.2	58.5±57.8
ALT ^a (IU/L)	63.8±28.0	80.4±48.4
GGT ^a (IU/L)	163±62	159±224
HbA1c ^a (%)	5.4±0.4	5.8±0.8
HOMA-IR ^a	1.7±0.6	3.8±2.9
Cholesterol ^{a, c} (mg/dL)	221±36	199±45
HDL ^a (mg/dL)	60±18	40±32
LDL ^a (mg/dL)	128±31	103±54
Triglycerides ^a (mg/dL)	169±95	244±309

BMI, body mass index; NAFL, non-alcoholic fatty liver; NASH, non-alcoholic steatohepatitis; PNPLA3, patatin-like phospholipase domain-containing protein 3; TM6SF2, transmembrane 6 superfamily 2; WHR, waist-to-hip ratio.

^aValues given as mean±SD.

^bSix patients were on a stable dose of metformin and two on simple diabetic diet.

^cTwo patients with NAFL and six with NASH were on statin therapy.

**P*<.05.

***P*<.01.

2.5 | MR-spectroscopy

MR spectroscopy was performed in fasting conditions, early in the morning within a 2-hour time frame prior to liver biopsy.

2.5.1 | ¹H-MRS

Hepatic steatosis and hepatic lipid composition were measured using single voxel PRESS sequence (TE=30 ms, TR=2000 ms, VOI: 3×3×3 cm³, six averages within acquisition time of 16 seconds during breathhold) at 3 T (Trio Tim; Siemens Healthcare, Erlangen, Germany) with the whole body RF coil for excitation and the combination of body-matrix and spine coil, supplied by system manufacturer, for signal acquisition. Representative spectra and typical VOI position are depicted in Figure 2 (panel A-C). Spectra were analyzed with AMARES within jMRUI¹⁵ and fat total signal area (FTSA—equal to hepatic steatosis) was assessed as the ratio of lipid signals (0.9–2.8 ppm) to the

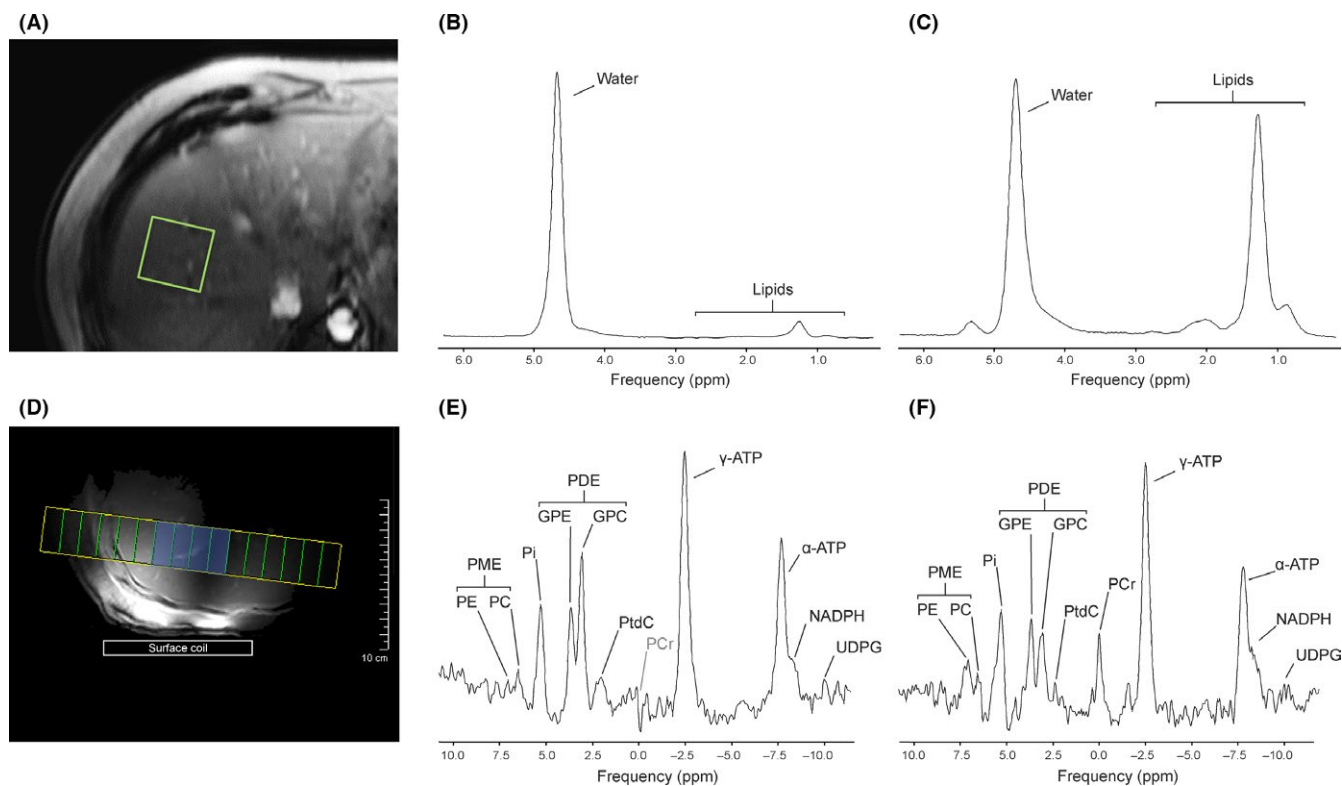


FIGURE 2 Magnetic resonance spectroscopy (MRS) procedure and representative ^1H and ^{31}P spectra of patients with non-alcoholic fatty liver disease (NAFL) and non-alcoholic steatohepatitis (NASH). The Volume of Interest for ^1H -MRS was placed in the right lobe of the liver (A). The different amounts of hepatic fat are illustrated by ^1H spectra from patient with NAFL and NASH (B, C respectively). The 2D chemical shift imaging (CSI) slice for ^{31}P -MRS was placed parallel to the RF surface coil carefully avoiding superficial skeletal muscle tissue (D). Signals from shaded voxels (4×4) were selected for processing and further analysis. The ^{31}P spectra from patients with NAFL (no/mild fibrosis) and NASH (advanced fibrosis) are depicted in E and F respectively. For illustration purposes, the ^{31}P spectra were filtered with 10 Hz Lorentzian filter. All amplitudes of the signals are in arbitrary units

whole ^1H MRS signal including that of water following appropriate T_1 and T_2 correction.

Lipid composition was assessed as lipid saturation (SI), unsaturation (UI), polyunsaturation (PUI) and monounsaturation (MUI) indices calculated as published before.⁶

2.5.2 | ^{31}P -MRS

For ^{31}P -MRS, the patients were placed in the right lateral position within a 7 T whole body MR system (Magnetom, Siemens Healthcare). Two dimensional ^{31}P -MR chemical shift imaging (CSI) sequence ($TE=1$ ms, $TR=1800$ ms, 12×12 matrix interpolated to 16×16 , FOV: 20×20 cm, four averages, acquisition time of approx. Ten minutes¹⁶ was applied on the 3 cm thick sagittal slice prescribed well in the liver parenchyma parallel to the RF surface coil ($^1\text{H}/^{31}\text{P}$, 10 cm in diameter, Rapid Biomedical GmbH, Rimpfing, Germany). Spectroscopic field of view was carefully chosen to avoid any contamination from a superficial skeletal muscle tissue (Figure 2D-F). From the ^{31}P MR signal, the amplitudes of phosphomonoester (PME) [phosphoethanolamine (PE)+phosphocholine], phosphodiester (PDE) [glycerophosphocholine (GPC)+glycerophosphoethanolamine], uridine-diphosphoglucose, nicotinic adenine dinucleotide phosphate (NADPH), inorganic phosphate

(Pi), phosphatidylcholine, α - and γ -adenosine triphosphate (ATP), phosphocreatine (PCr) and total phosphorus (TP) were determined as described before.^{17,18} VOI of 4×4 voxels with a sufficient signal-to-noise and no contamination from the skeletal muscle was chosen for further signal analysis. Individual phase and frequency shift correction was performed prior to a signal deconvolution with AMARES within jMRUI. Metabolite levels are expressed as ratio to TP or as ratio to γ -ATP signal following appropriate T_1 correction. At the end of measurement protocol, saturation transfer experiment was performed at the sagittal slab identical to the FOV of 2D CSI sequence. The chemical exchange rate constant k of the Pi-to-ATP reaction and the unidirectional forward exchange flux (F_{ATP}) were calculated as published before.¹⁹

2.6 | Liver biopsy and histology

Ultrasound assisted percutaneous liver biopsy was performed under local anaesthesia according to standard procedures²⁰ and in fasting condition. For histological analysis samples were routinely processed (formalin-fixed and paraffin-embedded), stained with haematoxylin/eosin and chrome aniline blue for assessment of fibrosis, steatosis and inflammation as well as with Prussian blue for iron.

Steatosis, ballooning, lobular inflammation and fibrosis were staged according to the *NASH Clinical Research Network Scoring System* definitions²¹: steatosis involving <5% of cells (S0, no steatosis), 5%–33% (S1, mild), >33%–66% (S2, moderate) and >66% (S3, severe) of hepatocytes; ballooning was graded as none (0), few balloon cells (1) and many cells/prominent ballooning (2); lobular inflammation was graded as no foci (0, none), <2 foci (1, mild), 2–4 foci (2, moderate) and >4 foci per 200× field (3, marked); fibrosis was staged as none (F0), perisinusoidal or periportal (F1), perisinusoidal and portal/periportal (F2), bridging fibrosis (F3) and cirrhosis (F4). The diagnosis of *non-alcoholic fatty liver* (NAFL) was made if steatosis was ≥5% and either ballooning or lobular inflammation or both were absent. The diagnosis of NASH was made given that: (i) steatosis was ≥5%, (ii) ballooning and lobular inflammation were present.²² Clinical differentiation was made for fibrosis stages 0–2 as no/mild fibrosis and for stages 3 and 4 as advanced fibrosis.

2.7 | Statistical analysis

Statistical analysis was performed with commercially available software (SPSS Version 23; IBM Corp., Chicago, IL, USA). Continuous variables were expressed as mean ± standard deviation while categorical variables as absolute (n) with relative frequencies (%). Comparison of continuous variables was calculated using the Student's *t*-test. Pearson's product moment correlation was used to calculate linear relationships between variables. Categorical variables were compared using the analysis of variance (ANOVA). Binary logistic regression was used where appropriate. Factors showing significant association in univariate analysis were also included into a multivariate model. Multivariate analysis was performed for F_{ATP} and k including BMI, waist-to-hip ratio (WHR), hepatic steatosis and the presence of diabetes for the discrimination of NAFL and NASH. All tests were two-sided with a *P*-value below .05 as level of significance.

3 | RESULTS

3.1 | Patients' characteristics

Thirty patients with NAFLD undergoing liver biopsy between 2010 to 2013 were included in this study (Figure 1), eight of them with NAFL and 22 with NASH (clinical characteristics see Table 1). No difference between sex and age was observed between both groups. NASH patients had a significantly higher BMI and WHR. Non-obese (BMI<30) and obese (BMI>30) NAFLD patients were equally distributed with no significant difference between NAFL and NASH. In this cohort, only patients with NASH had diabetes. Concomitant anti-diabetic therapy included metformin in six patients and diabetic diet only in two patients. Eight patients had statin therapy without statistical differences between the two groups. In addition, there was no significant difference in serum cholesterol or HOMA index. The contribution of the PNPLA3 rs738409 polymorphism was only significantly different between NASH and NAFL for genotype GG (148M/M) (*P*=.003), which was not significant for TM6SF2 variants. Histology data is shown in Table 2.

TABLE 2 Histological characteristics of the subject cohort

	NAFL (n=8) ^a	NASH (n=22)
Steatosis ^b (%)	15±10	65±24**
Ballooning ^b	0.8±0.7	1.3±0.6*
Lobular inflammation ^a	0.60±0.52	1.40±0.50**
Fibrosis ^a (Kleiner)	0.5±0.5	1.8±1.2**
NAS ^a	2.25±1.10	5.30±1.40**
Fibrosis grade 3/4 (%)	0 (0)	6 (27)
Cirrhosis (%)	0 (0)	3 (14)

NAFL, non-alcoholic fatty liver; NASH, non-alcoholic steatohepatitis.

Patients diagnosed with non-alcoholic steatohepatitis NASH in histology needed at least one point for ballooning and lobular inflammation, respectively, with grade 1 or higher in hepatic steatosis.²²

^aIncluding four patients with possible borderline NASH (= grade 1–2 ballooning without lobular inflammation or grade 1–2 lobular inflammation without ballooning).

^bValues given as mean ± standard deviation.

**P*<.05.

***P*<.01.

3.2 | ¹H MRS

Steatosis as calculated from ¹H-MRS at 3 T highly correlated with histological steatosis (*r*=.716, *P*<.001) (Figure 3) and lobular inflammation (*r*=.420, *P*=.021). Steatosis in MRS also correlated with BMI (*r*=.506, *P*=.004), serum triglycerides (*r*=.444, *P*=.014) but not cholesterol or diabetes. Serum high-density lipoprotein (HDL) levels highly decreased with increasing degree of steatosis in MRS (*r*=−0.550, *P*=.002). Notably, we observed no differences between NAFL and NASH in lipid composition measured as lipid saturation (SI), polyunsaturation (PUI) and monounsaturations (MUI) indices, however, PUI to MUI ratios were significantly higher in non-obese (BMI<30) than obese (BMI>30) individuals (*P*=.025). ¹H-MRS showed higher PUI in PNPLA3 genotype GG (*r*=.423; *P*=.02). Importantly, NASH patients showed significantly higher degrees of steatosis on MRS cross-validated by liver histology compared to NAFL (*P*<.001; Figure 3). There was no correlation between genotype GG and steatosis. However, steatosis negatively correlated with genotype CC (*P*=.023). No correlation was found within TM6SF2 variants.

3.3 | ³¹P MRS

3.3.1 | Phosphomonoesters and phosphodiester

PE/(PME+PDE) (*P*=.04), PE/γ-ATP (*P*=.002) and PE/TP (*P*=.015) ratios as markers of cell membrane turnover were lower in patients with no/mild fibrosis (F0–2) than advanced fibrosis F3–4. This was also observed for PME/γ-ATP ratios (*P*=.013). Inversely, GPC/(PME+PDE) ratios (*P*=.05) as cell membrane breakdown products were higher in no-to-mild fibrosis compared to advanced fibrosis (Figure 4). There was no correlation with lobular inflammation but slightly higher PME/TP ratios in grade 2 ballooning than in grade 1 (grade 2>1; *P*=.015) without difference to grade 0 (grade 1>0; *P*=.28).

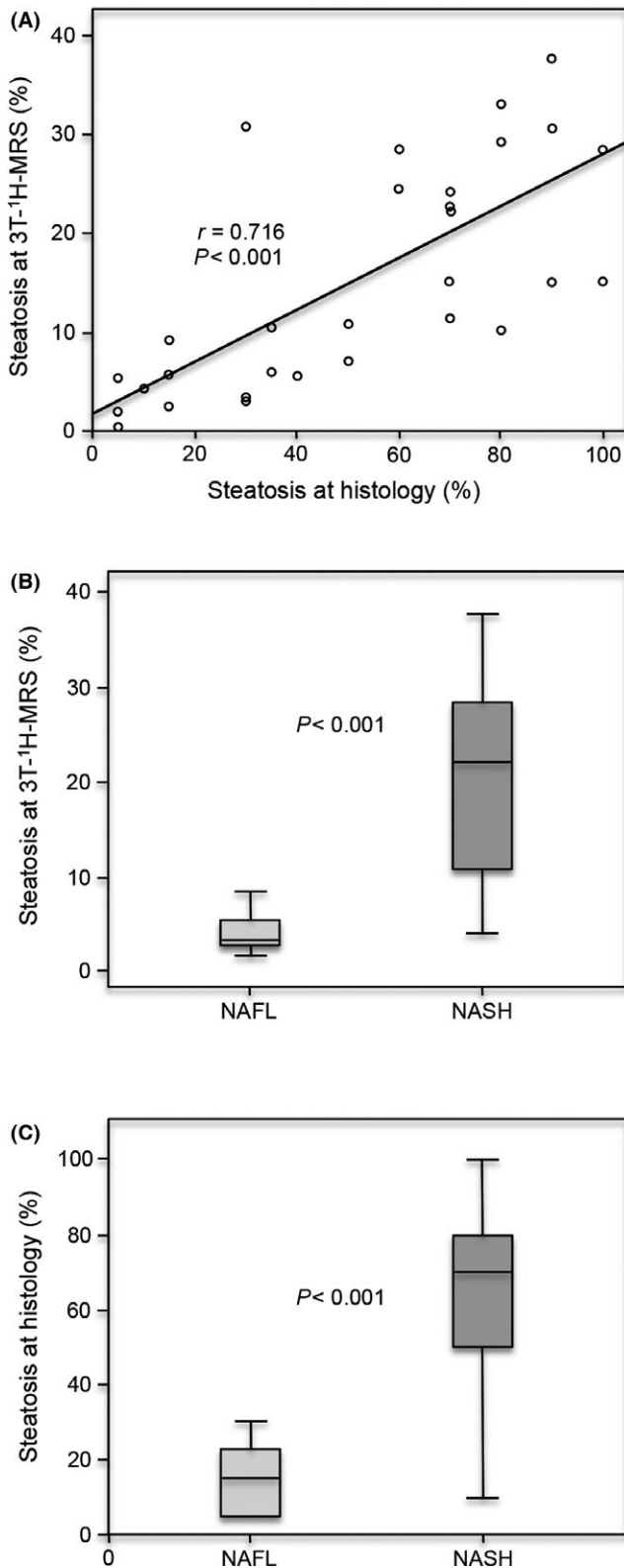


FIGURE 3 Hepatic fat fraction in non-alcoholic fatty liver disease (NAFL) and non-alcoholic steatohepatitis (NASH) assessed with ^1H -MRS and liver histology. (A) High correlation of lipid content on liver histology as gold standard with $3\text{ T } ^1\text{H}$ -MRS ($r=0.716$, $P<0.001$). NASH patients show a higher hepatic fat fraction on (B) $3\text{ T } ^1\text{H}$ -MRS ($P<0.001$), which was also confirmed by (C) histology ($P<0.001$)

3.3.2 | ATP, inorganic phosphate, phosphocreatine and NADPH

$\gamma\text{-ATP/TP}$ ($P=0.049$) ratio as marker of hepatic energy metabolism decreased from F0-2 to F3-4. $\text{PCr}/\gamma\text{-ATP}$ ($P=0.002$) and PCr/TP ($P=0.014$) ratios conversely increased in patients with advanced fibrosis after multivariate analysis for the presence of diabetes. $\text{NADPH}/(\text{PME}+\text{PDE})$ ($P=0.048$), $\text{NADPH}/\gamma\text{-ATP}$ ($P=0.028$) and NADPH/TP ($P=0.026$) ratios were higher in grade 0 to 2 ballooning rising from few (grade 1) to many ballooned cells (grade 2) ($P=0.05$) in NADPH/TP (Figure 5). There was no significant difference between diabetic and non-diabetic individuals in ATP, PCr or NADPH. Contamination of hepatic ^{31}P -MRS signal by the signal from superficial skeletal muscle was minimized by the choice of MRSI field of view, prescribed as sagittal slice parallel to the surface coil, placed well within liver parenchyma (Figure 2D) and acquisition frequency centred to PCr resonance position, leading to no chemical shift displacement artefact. Subsequently, VOI was carefully selected during signal processing, ensuring that our spectra were not affected by the signals from skeletal muscle.

3.3.3 | Saturation transfer: forward exchange flux and exchange rate constant

Mean k values assessing mitochondrial function were significantly lower in patients with NASH ($0.20\pm 0.07/\text{seconds}$) than in those with NAFL ($0.30\pm 0.07/\text{seconds}$; $P=0.003$). NASH patients had also lower estimated F_{ATP} values ($0.21\pm 0.08\text{ mM/seconds}$) than NAFL patients ($0.38\pm 0.08\text{ mM/seconds}$; $P<0.001$) (Figure 6) and were both still significant after multivariate analysis for BMI, the presence of diabetes and adjusting for steatosis. There was no correlation with ballooning in histology but a strong correlation of lobular inflammation to both k values ($P=0.007$) and F_{ATP} values ($P<0.001$). In addition, a minor correlation was found for F_{ATP} and steatosis measured by histology ($P=0.03$) and $3\text{ T } ^1\text{H}$ -MRS ($P=0.021$).

4 | DISCUSSION

To our best knowledge, this is the first prospective clinical trial evaluating overall hepatic ($3\text{ T } ^1\text{H}$ - and $7\text{ T } ^{31}\text{P}$ -MR spectroscopy (MRS) profiles including dynamic saturation transfer technique in biopsy proven NAFLD patients uncovering important metabolic differences between NAFL and NASH.

Hepatic steatosis as determined by $3\text{ T } ^1\text{H}$ -MRS highly correlated with histological steatosis. As ^1H -MRS quantifies the relative amount of fat in the entire region of interest and histology states the fraction of steatotic liver cells a direct comparison regarding quantification of fat might not be advantageous. However, using a linear regression model as described before²³ an approximation to histology is possible even though not implicitly required considering the well known shortcomings of liver histology regarding fat quantification. In this cohort, hepatic fat in ^1H -MRS and histology was higher in NASH patients than

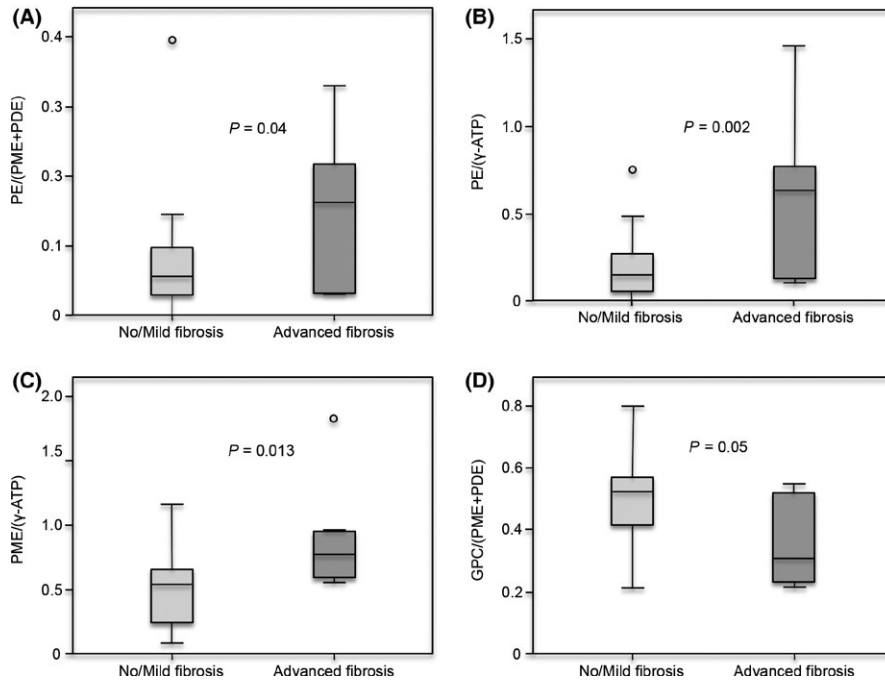


FIGURE 4 ^{31}P -MRS:

Phosphomonoesters and phosphodiester uncover alterations in cell membrane metabolism in non-alcoholic fatty liver disease (NAFLD). Phosphomonoesters like phosphoethanolamine (PE) were significantly higher in advanced fibrosis than no-to-mild fibrosis: (A) PE/phosphomonoester (PME)+phosphodiester (PDE) ($P=.04$), (B) PE/ γ -adenosine triphosphate (ATP) ($P=.002$) and (C) PME/ γ -ATP ($P=.013$). (D) This was reversed for phosphodiester like glycerophosphocholine (GPC)/(PME+PDE) ($P=.05$). ^{31}P -MRS shows alterations in cell membrane metabolism in advanced NAFLD with higher degree of fibrosis

in patients with NAFL. In addition, lobular inflammation correlated with hepatic fat in MRS. This supports recent data from the NASH Clinical Research Network²⁴ showing significant correlations between increasing levels of steatosis and diagnosis of NASH.

Lipid saturation with higher prevalence of potentially more toxic unsaturated fatty acids may be a critical determinant of lipotoxicity.²⁵ We therefore used ^1H -MRS to assess lipid saturation profiles (ie, SI, UI, MUI, PUI) but observed no differences between NAFL and NASH, non-diabetics and diabetics or different stages of fibrosis. Interestingly, hepatic PUI to MUI ratios were significantly higher in non-obese ($\text{BMI}<30$) than obese ($\text{BMI}>30$) NAFLD patients. Notably, our results are in line with hepatic lipidomic analysis of NAFLD showing no difference between NAFL and NASH.²⁶ In addition, hepatic PUI was increased in homozygous carriers of the PNPLA3 I148M variant (G/G), which may be considered as a specific subtype of NASH²⁷ but not in any TM6SF2 variant.

NAFLD/NASH is a condition possibly characterized by ER stress.²⁸ We tested the hypotheses that ultra-high field ^{31}P -MRS may uncover alterations in phospholipid metabolites such as PME and PDE previously prescribed as markers of hepatic endoplasmic stress.²⁹ However, we did not observe any differences in PMEs and PDEs possibly due to a higher differentiation of the PME and PDE signals at 7 T. Levels of PE were lower in no-to-mild than in advanced fibrosis, which was also reflected by PME/ γ -ATP ratios. Inversely, GPC/(PME+PDE) ratios were higher in advanced fibrosis supporting former data.³⁰ Our results reflect alterations in cell membrane metabolism in advanced NASH as described in diffuse liver disease,³¹ fibrosis and cirrhosis.³²

In this study, we uncovered decreased ratios of γ -ATP/TP in advanced fibrosis indicating a disturbed energy metabolism in advanced steatohepatitis. Decreasing concentrations of hepatic ATP were also shown in patients with type 2 diabetes³³ which could not be shown in our cohort. Nevertheless, multivariate analysis was performed

adjusting for possible effects of diabetes, BMI and WHR on hepatic energy metabolism, not changing the original findings.

Previous studies uncovered hepatic mitochondrial structural defects and functional mitochondrial abnormalities in NASH.^{17,34} This may indicate that changes in hepatic energy homeostasis and increased oxidative stress in NASH could promote cell injury and inflammation. In this study, PCr/ γ -ATP and PCr/TP ratios increase with advanced fibrosis supporting the concept of dysfunctional mitochondria in advanced NASH.^{10,35} To exclude contamination of hepatic ^{31}P -MRSI data by signals from skeletal muscle, we carefully analyzed our acquisition scheme and compared presented data post hoc with data from healthy volunteers partially published before.¹⁸ The retrospective analysis of these identically acquired spectra¹⁸ from young healthy volunteers ($n=9$) yielded mean PCr/TP signal of 0.010 ± 0.007 similar to data from patients with no or mild fibrosis from this study. Collectively, this strongly supports that the statistical increase in PCr/TP signal from liver of patients with advanced fibrosis represents real presence of PCr in the measured volume. So far, no other study on MR spectroscopy in NAFLD or diabetes has shown the presence of PCr signals, which might be explained by the higher resolution of ultra-high field MR at 7 T. Therefore, interpretation of these findings should be done with caution, until confirmed in larger studies.

Although PCr is usually not present in normal hepatocytes and healthy liver,³⁶ creatine kinase (CK) activities in endothelial cells, Kupffer and Ito cells could be shown in several in vivo and in vitro experimental models.³⁷ Our results might be therefore explained by a compensatory up-regulation of CK expression in advanced NASH with more advanced fibrosis due to a dysfunctional hepatic microvasculature³⁸ and hypoxia.³⁹ NADPH additionally increased with higher grades of hepatocellular ballooning possibly reflecting higher oxidative activity during inflammation⁴⁰ formerly shown in NASH.³⁰

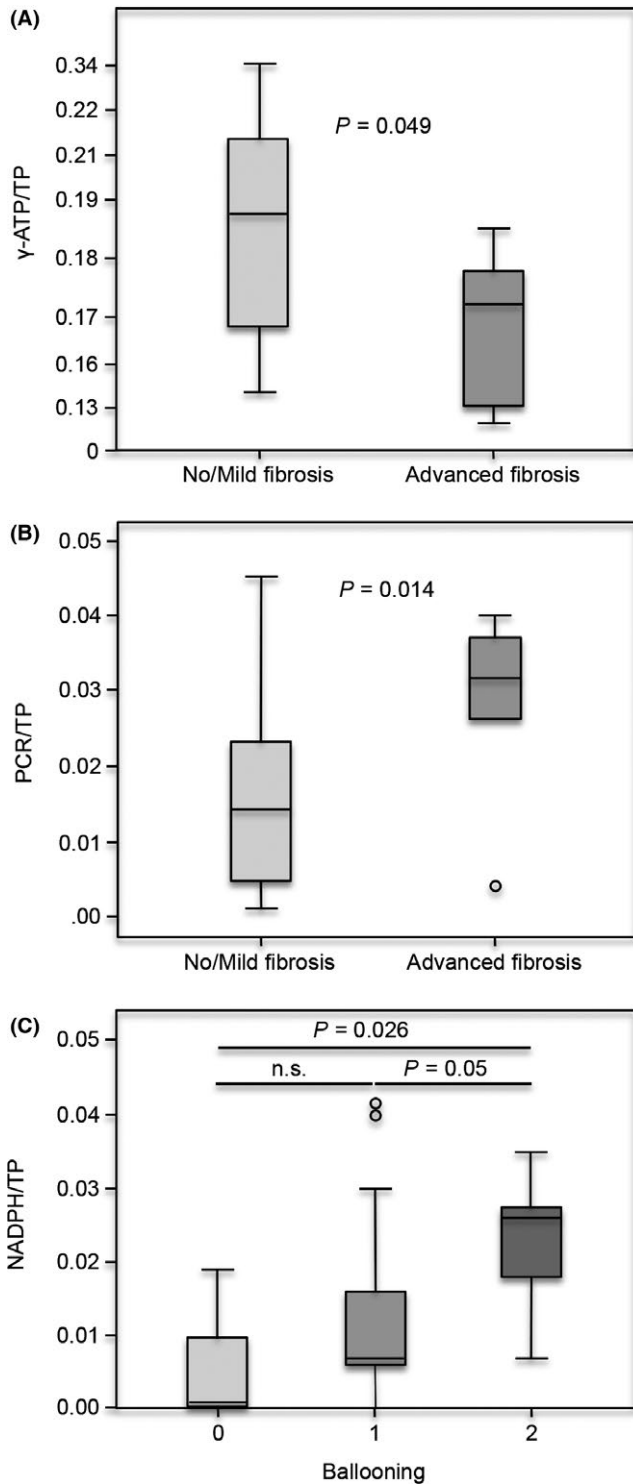


FIGURE 5 ^{31}P -MRS: adenosine triphosphate (ATP), inorganic phosphate, phosphocreatine and nicotinamide adenine dinucleotide phosphate (NADPH) reflecting altered energy metabolism in non-alcoholic fatty liver disease (NAFLD). ^{31}P -MRS data show an altered hepatic energy metabolism in higher grades of fibrosis in NAFLD patients. (A) Advanced fibrosis showed lower levels of γ -adenosine triphosphate (ATP)/total phosphorus (TP) ($P=0.049$). (B) Conversely phosphocreatine (PCr)/TP increased in advanced fibrosis ($P=0.014$). (C) NADPH/TP ratios increased with higher grades of ballooning (no (0) vs many ballooned cells (2), $P=0.028$; few (1) vs many ballooned cells (2), $P=0.05$). Choice of spectroscopic field of view, which can be described as sagittal slab parallel to the surface coil, placed well within liver parenchyma (Figure 2D), acquisition frequency centred to PCr resonance position, leading to no chemical shift displacement artefact, and careful volume of interest (VOI) selection during signal processing, all supports the valid assumption, that our spectra are not contaminated by the signals from skeletal muscle

Finally, we used the saturation transfer technique to assess dynamic Pi-to-ATP exchange parameters in NAFL and NASH, which was already used to monitor changes in the Pi-to-ATP flux reflecting alterations in the mitochondrial metabolism in the human muscle⁴¹ not shown for liver tissue so far. The exchange rate constant k and the unidirectional forward exchange flux F_{ATP} were significantly lower in patients with NASH than with NAFL even after correction for the effects of diabetes, BMI and steatosis emphasizing our pilot study results¹⁹ in showing a disturbed energy metabolism in NASH. Both, increased

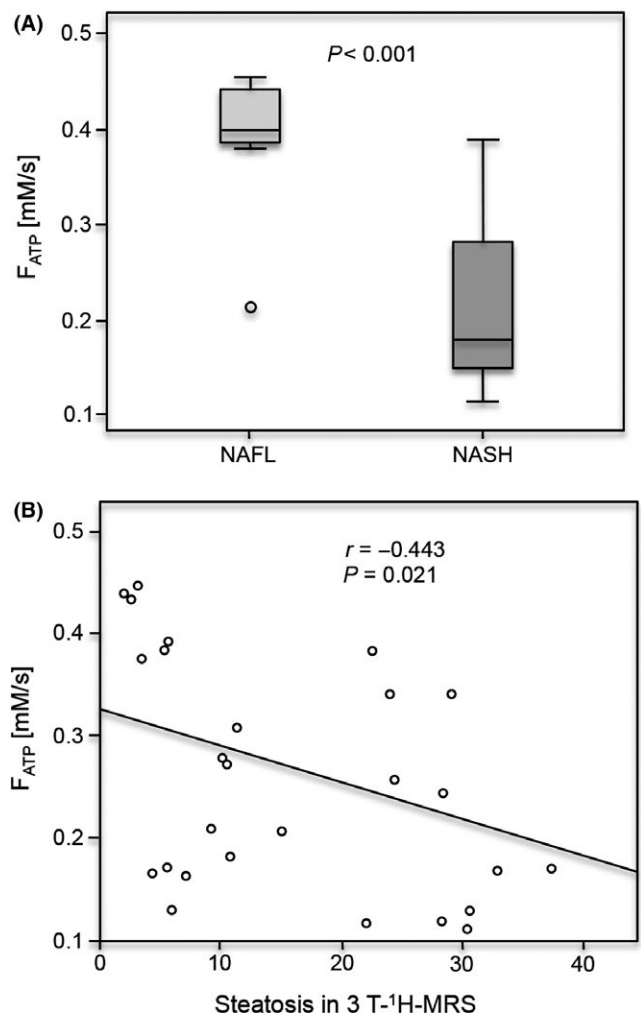


FIGURE 6 Saturation transfer ^{31}P -MRS: Higher adenosine triphosphate (ATP) fluxes in non-alcoholic fatty liver disease (NAFLD) than non-alcoholic steatohepatitis (NASH). (A) Forward exchange flux (F_{ATP}) was lower in patients with NASH (0.21 ± 0.08 mM/s) than with non-alcoholic fatty liver (NAFL) (0.38 ± 0.08 mM/s) consistent with abnormal mitochondrial function ($r = -.679$; $P < .001$). (B) In addition a minor correlation was also found for F_{ATP} and steatosis in 3-T ^1H -MRS ($r = -.443$; $P = .021$)

fatty acid β -oxidation and hepatic oxidative stress are common in NAFLD.³⁴ However, a loss of adaptive mechanisms in mitochondrial function and mitochondrial structural defects has only been associated with NASH^{7,10,34} and progressive impairment of the mitochondrial respiratory capacity may play a pivotal role in the progression of NASH.⁴² To illustrate the potential application of dynamic saturation transfer, we performed a small pilot case series of three patients who underwent ¹H- and ³¹P-MRS 12 months after a dietary intervention (Figure S1) showing regenerating Pi-to-ATP exchange parameters when hepatic steatosis improved (n=2) while revealing further impairment of Pi-to-ATP exchange parameters in case (n=1) of increasing hepatic steatosis, which at this point is rather preliminary and speculative until more extensively investigated.

As limitations of our study we have to acknowledge that the sample volume of liver biopsies and the region of interest measured by MRS are different, which is due to technique limitations in liver biopsy. This study was planned as a pilot study to evaluate the feasibility of extended high and ultra-high field ¹H- and ³¹P-MRS profiles in NAFLD patients and therefore the sample size is relatively small. We are aware, that the best possible internal reference and the measure of energy metabolism would be the β -ATP resonance, but limited spectral bandwidth of slice selective radio frequency pulses does not allow for effective excitation of β -ATP signal at 7 Tesla. For this technical reason, γ -ATP was chosen as the surrogate marker of energy metabolism. Furthermore, there is a possible selection bias towards patients with more advanced disease due to the requirements for routine liver biopsy indication. Conversely, the subjects characterized by NAFL were clustered in a rather low range of the steatosis scale. However, a major strength of this study is the exact timeline with short intervals and constant fasting conditions at which MRS and liver biopsy were conducted.

In conclusion, 3 T ¹H- and 7 T ³¹P-MRS are highly accurate and fast non-invasive methods, generating broad in vivo lipid, cell membrane and energy metabolism profiles of the human liver. Ultra-high field MRS at 7 Tesla with higher spectral resolution and increased signal-to-noise ratios leads to shorter acquisition times and may therefore improve clinical applicability in a tertiary (research) setting. Dynamic saturation transfer including ATP flux shows significant differences in hepatic energy metabolism between NAFL and NASH with compensatory increasing ratios of phosphocreatine supporting data on apparent mitochondrial structure defects in NASH. 3 T ¹H- and 7 T ³¹P-MRS may allow non-invasive metabolic profiling assisting further mechanistic and therapeutic studies of NAFLD/NASH.

CONFLICT OF INTEREST

MT serves as a consultant for Albireo, Falk, Genfit, Gilead, Intercept, MSD, Novartis and Phenex and is a member of the speakers' bureau of Falk, Gilead, MSD and Roche. He further received travel grants from Falk, Roche and Gilead and unrestricted research grants from Albireo, Falk, Intercept and MSD. He is also co-inventor of a patent on the medical use of nor-UDCA. All other authors have no financial disclosures concerning this study to report.

REFERENCES

- Williams CD, Stengel J, Asike MI, et al. Prevalence of nonalcoholic fatty liver disease and nonalcoholic steatohepatitis among a largely middle-aged population utilizing ultrasound and liver biopsy: a prospective study. *Gastroenterology*. 2011;140:124-131.
- Nalbantoglu I, Brunt EM. Role of liver biopsy in nonalcoholic fatty liver disease. *World J Gastroenterol*. 2014;20:9026-9037.
- Thomsen C, Becker U, Winkler K, Christoffersen P, Jensen M, Henriksen O. Quantification of liver fat using magnetic resonance spectroscopy. *Magn Reson Imaging*. 1994;12:487-495.
- Ruiz-Cabello J, Cohen JS. Phospholipid metabolites as indicators of cancer cell function. *NMR Biomed*. 1992;5:226-233.
- Krassak M, Hofer H, Wrba F, et al. Non-invasive assessment of hepatic fat accumulation in chronic hepatitis C by 1H magnetic resonance spectroscopy. *Eur J Radiol*. 2010;74:e60-e66.
- Johnson NA, Walton DW, Sachinwalla T, et al. Noninvasive assessment of hepatic lipid composition: advancing understanding and management of fatty liver disorders. *Hepatology*. 2008;47:1513-1523.
- Koliaki C, Szendroedi J, Kaul K, et al. Adaptation of hepatic mitochondrial function in humans with non-alcoholic fatty liver is lost in steatohepatitis. *Cell Metab*. 2015;21:739-746.
- Befroy DE, Perry RJ, Jain N, et al. Direct assessment of hepatic mitochondrial oxidative and anaplerotic fluxes in humans using dynamic 13C magnetic resonance spectroscopy. *Nat Med*. 2014;20:98-102.
- Abrigo JM, Shen J, Wong VW-S, et al. Non-alcoholic fatty liver disease: spectral patterns observed from an in vivo phosphorus magnetic resonance spectroscopy study. *J Hepatol*. 2014;60:809-815.
- Koliaki C, Roden M. Hepatic energy metabolism in human diabetes mellitus, obesity and non-alcoholic fatty liver disease. *Mol Cell Endocrinol*. 2013;379:35-42.
- Kraff O, Fischer A, Nagel AM, Monninghoff C, Ladd ME. MRI at 7 Tesla and above: demonstrated and potential capabilities. *J Magn Reson Imaging*. 2015;41:13-33.
- Romeo S, Kozlitina J, Xing C, et al. Genetic variation in PNPLA3 confers susceptibility to nonalcoholic fatty liver disease. *Nat Genet*. 2008;40:1461-1465.
- Singal AG, Manjunath H, Yopp AC, et al. The effect of PNPLA3 on fibrosis progression and development of hepatocellular carcinoma: a meta-analysis. *Am J Gastroenterol*. 2014;109:325-334.
- Liu YL, Reeves HL, Burt AD, et al. TM6SF2 rs58542926 influences hepatic fibrosis progression in patients with non-alcoholic fatty liver disease. *Nat Commun*. 2014;5:4309.
- Vanhamme L, van den Boogaart A, van Huffel S. Improved method for accurate and efficient quantification of MRS data with use of prior knowledge. *J Magn Reson*. 1997;129:35-43.
- Chmelik M, Kukurova IJ, Gruber S, et al. Fully adiabatic 31P 2D-CSI with reduced chemical shift displacement error at 7 T-GOIA-1D-ISIS/2D-CSI. *Magn Reson Med*. 2013;69:1233-1244.
- Cortez-Pinto H, Chatham J, Chacko VP, Arnold C, Rashid A, Diehl AM. Alterations in liver ATP homeostasis in human nonalcoholic steatohepatitis: a pilot study. *JAMA*. 1999;282:1659-1664.
- Chmelik M, Schmid AI, Gruber S, et al. Three-dimensional high-resolution magnetic resonance spectroscopic imaging for absolute quantification of 31P metabolites in human liver. *Magn Reson Med*. 2008;60:796-802.
- Valkovic L, Gajdosik M, Traussnigg S, et al. Application of localized (3)(1)P MRS saturation transfer at 7 T for measurement of ATP metabolism in the liver: reproducibility and initial clinical application in patients with non-alcoholic fatty liver disease. *Eur Radiol*. 2014;24:1602-1609.
- Strassburg CP, Manns MP. Approaches to liver biopsy techniques-revisited. *Semin Liver Dis*. 2006;26:318-327.
- Kleiner DE, Brunt EM, van Natta M, et al. Design and validation of a histological scoring system for nonalcoholic fatty liver disease. *Hepatology*. 2005;41:1313-1321.

22. Bedossa P, Poitou C, Veyrie N, et al. Histopathological algorithm and scoring system for evaluation of liver lesions in morbidly obese patients. *Hepatology*. 2012;56:1751-1759.
23. Hájek M, Dezortová M, Wagnerová D, et al. MR spectroscopy as a tool for in vivo determination of steatosis in liver transplant recipients. *MAGMA*. 2011;24:297-304.
24. Chalasani N, Wilson L, Kleiner DE, et al. Relationship of steatosis grade and zonal location to histological features of steatohepatitis in adult patients with non-alcoholic fatty liver disease. *J Hepatol*. 2008;48:829-834.
25. Fuchs CD, Claudel T, Trauner M. Role of metabolic lipases and lipolytic metabolites in the pathogenesis of NAFLD. *Trends Endocrinol Metab*. 2014;25:576-585.
26. Puri P, Baillie RA, Wiest MM, et al. A lipidomic analysis of nonalcoholic fatty liver disease. *Hepatology*. 2007;46:1081-1090.
27. Yki-Jarvinen H. Non-alcoholic fatty liver disease as a cause and a consequence of metabolic syndrome. *Lancet Diabetes Endocrinol*. 2014;2:901-910.
28. Zhang XQ, Xu CF, Yu CH, Chen WX, Li YM. Role of endoplasmic reticulum stress in the pathogenesis of nonalcoholic fatty liver disease. *World J Gastroenterol*. 2014;20:1768-1776.
29. Menon DK, Harris M, Sargentoni J, Taylor-Robinson SD, Cox IJ, Morgan MY. In vivo hepatic ³¹P magnetic resonance spectroscopy in chronic alcohol abusers. *Gastroenterology*. 1995;108:776-788.
30. Sevastianova K, Hakkarainen A, Kotronen A, et al. Nonalcoholic fatty liver disease: detection of elevated nicotinamide adenine dinucleotide phosphate with in vivo 3.0-T ³¹P MR spectroscopy with proton decoupling. *Radiology*. 2010;256:466-473.
31. van Wassenae-van Hall HN, van der Grond J, van Hattum J, Kooijman C, Hoogenraad TU, Mali WP. ³¹P magnetic resonance spectroscopy of the liver: correlation with standardized serum, clinical, and histological changes in diffuse liver disease. *Hepatology*. 1995;21:443-449.
32. Noren B, Forsgren MF, Dahlgqvist Leinhard O, et al. Separation of advanced from mild hepatic fibrosis by quantification of the hepatobiliary uptake of Gd-EOB-DTPA. *Eur Radiol*. 2013;23:174-181.
33. Szendroedi J, Chmelik M, Schmid AI, et al. Abnormal hepatic energy homeostasis in type 2 diabetes. *Hepatology*. 2009;50:1079-1086.
34. Sanyal AJ, Campbell-Sargent C, Mirshahi F, et al. Nonalcoholic steatohepatitis: association of insulin resistance and mitochondrial abnormalities. *Gastroenterology*. 2001;120:1183-1192.
35. Sunny NE, Parks EJ, Browning JD, Burgess SC. Excessive hepatic mitochondrial TCA cycle and gluconeogenesis in humans with nonalcoholic fatty liver disease. *Cell Metab*. 2011;14:804-810.
36. Meffert G, Gellerich FN, Margreiter R, Wyss M. Elevated creatine kinase activity in primary hepatocellular carcinoma. *BMC Gastroenterol*. 2005;5:9.
37. Vaubourdolle M, Chazouilleres O, Poupon R, et al. Creatine kinase-BB: a marker of liver sinusoidal damage in ischemia-reperfusion. *Hepatology*. 1993;17:423-428.
38. McCuskey RS, Ito Y, Robertson GR, McCuskey MK, Perry M, Farrell GC. Hepatic microvascular dysfunction during evolution of dietary steatohepatitis in mice. *Hepatology*. 2004;40:386-393.
39. Nath B, Szabo G. Hypoxia and hypoxia inducible factors: diverse roles in liver diseases. *Hepatology*. 2012;55:622-633.
40. de Minicis S, Bataller R, Brenner DA. NADPH oxidase in the liver: defensive, offensive, or fibrogenic? *Gastroenterology*. 2006;131:272-275.
41. Befroy DE, Rothman DL, Petersen KF, Shulman GI. ³¹P-magnetization transfer magnetic resonance spectroscopy measurements of in vivo metabolism. *Diabetes*. 2012;61:2669-2678.
42. Begriche K, Igoudjil A, Pessayre D, Fromenty B. Mitochondrial dysfunction in NASH: causes, consequences and possible means to prevent it. *Mitochondrion*. 2006;6:1-28.

SUPPORTING INFORMATION

Additional Supporting Information may be found online in the supporting information tab for this article.

How to cite this article: Traussnigg S, Kienbacher C, Gajdošik M, et al. Ultra-high-field magnetic resonance spectroscopy in non-alcoholic fatty liver disease: Novel mechanistic and diagnostic insights of energy metabolism in non-alcoholic steatohepatitis and advanced fibrosis. *Liver Int*. 2017;37:1544-1553. <https://doi.org/10.1111/liv.13451>